Available online at www.sciencedirect.com
ScienceDirect
Electrochimica Acta 52 (2007) 2229–2235
ELECTROCHIMICA Acta
www.elsevier.com/locate/electacta

Potential-induced lifting of the Au(1 0 0)-surface reconstruction studied with DFT

Timo Jacob

Fritz-Haber-Institut der Max-Planck-Gesellschaft, Faradayweg 4-6, D-14195 Berlin, Germany

Received 1 February 2006; received in revised form 14 March 2006; accepted 14 March 2006
Available online 13 October 2006

Abstract

The potential-induced surface reconstruction of Au(1 0 0) was studied by a combination of density functional theory (DFT) and thermodynamic considerations. On the basis of realistic models for the reconstructed surface ((5 × 1) and (7 × 1) unitcells), in which a hexagonal overlayer was located above the bulk-truncated Au(1 0 0) surface, we found that applying an electric field causes a slight lifting of the overlayer, leading to a stronger surface buckling than without electric field. Using experimental cyclovoltammetry measurements we were able to relate the electric field applied in our calculations to the electrode potential. The resulting surface free energy curves showed a transition from the hexagonal-reconstructed surface phase to the non-reconstructed structure between +0.5 and +0.6 V (versus SCE-electrode) depending on the ion concentration in the electrolyte. Higher potentials values are required at lower electrolyte concentrations.

Keywords: Density functional theory; Au; Surface-reconstruction; Electrochemistry

1. Introduction

Under ultra-high vacuum (UHV) conditions some low-index surfaces of the late 5d metals Au, Pt, and Ir show a reconstruction of the first surface layer. In order to maximize the number of surface bonds, the ground state of the (1 0 0) face corresponds to a quasihexagonal (hex) close-packed structure, which results in an overall lower surface free energy. Especially the reconstruction of Au(1 0 0) has intensively been studied by experiment and theory. As nicely summarized in Refs. [1,2], from low-electron diffraction (LEED) and helium diffraction experiments first a (1 × 5) and later a (20 × 15) reconstruction has been proposed [3–5]. However, further LEED studies [6,7] suggested a $c(26 \times 68)$ reconstruction, while even more complex structures were found by scanning tunnelling microscopy (STM) [8]. In order to explain the structure of the reconstructed surface several theoretical work can be found in literature ranging from tight-binding approaches [9] over simple glue models [10] to the application of embedded atom potentials [11] and even first-principle calculations [12].

Besides changing the surface morphology by heat-treatment, the potential-induced reconstruction has become a topic of interest in electrochemistry. On the basis of different surface sensitive techniques and cyclovoltammetry experiments (CV) Kolb and coworkers [1,13–15] found that the Au(1 0 0)-hex structure, which is the ground state under UHV conditions, is stable below +0.55 V (versus SCE—saturated calomel electrode) when being in contact with a 0.01 M $HClO_4$ electrolyte. Since the first surface layer is close-packed, the measured capacity curve was found to be comparable with the one obtained for Au(1 1 1). However, if more positive potentials were applied a removal of the reconstruction (*lifting*) could be observed, leading to the non-reconstructed Au(1 0 0)-(1 × 1) surface structure. If after lifting the reconstruction the potential is decreased from a value above +0.55 to −0.25 V the surface changes back to the reconstructed Au(1 0 0)-hex structure, which can be seen by the behavior of the corresponding CV-curve. Although the back-transition seems to involve an energetic barrier, the hex ↔ (1 × 1) transition is highly reversible. Hence, it has become a question whether the lifting of the surface reconstruction is due to surface charging (as a result of the electrode potential), adsorption of electrolyte ions, or even both.

Assuming a simple capacitor model for the electric double-layer, Santos and Schmickler [16] used experimentally measured capacity curves for different electrolyte concentrations to evaluate the surface free energy γ for reconstructed

0013-4686/$ – see front matter © 2006 Elsevier Ltd. All rights reserved.
doi:10.1016/j.electacta.2006.03.114

and unreconstructed surfaces of Au(1 0 0) and Au(1 1 1). At around +0.6 V they found an intersection between $\gamma_{\mathrm{Au(1\,0\,0)\text{-}hex}}$ and $\gamma_{\mathrm{Au(1\,0\,0)\text{-}(1\times1)}}$ and concluded that positive excess charge on the surface is responsible for the lifting of reconstruction in the case of weakly adsorbing electrolytes. They also evaluated the influence of the electrolyte concentration on the capacitance.

Haftel [17] used the embedded atom method (EAM) for the study of structure and dynamics of metallic systems and investigated the surface reconstructions of various faces of Au and Pt theoretically with a number of different interaction potentials. Later, Haftel and Rosen [18,19] employed the surface embedded atom method (SEAM) to calculate the total energy of Au(1 0 0)-hex, Au(1 0 0)-(1 × 1), and Au(1 1 1)-(1 × 1). In order to account for the electrode potential, they added additional charge to the atoms at the electrode surface. From their studies, they concluded that surface charge plays an important role in the lifting of reconstruction. In addition, they estimated the reconstruction energy as function of change in surface strain and found this factor to be important only for higher potentials.

While in previous *ab initio* studies the reconstructed surface was mostly simulated as Au(1 1 1), recently Feng et al. [20] performed periodic DFT calculations on the realistic system in which they used a (5 × 1) unitcell and added an additional atom to the first surface layer. In their calculations the electrode potential was included by charging the slab and placing a reference electrode (with the counter charge) in the middle of the vacuum region. From the surface free energies-curves, which were evaluated on the basis of experimentally measured capacitancies, they concluded that there is no necessity for specific ion adsorption [21] and that only the positive surface charge would already be sufficient for lifting of reconstruction.

Following the approach suggested by Feng et al. in this paper we present *ab initio* DFT calculations on the Au(1 0 0)-(1 × 1) and Au(1 0 0)-hex surfaces, but now applying an external electric field to account for the electrode potential. The reconstructed surface is modeled with two different surface unitcells, which show only a small mismatch to the periodicity of the underlying structure. Finally, in order to obtain surface free energies as function of electrode potential a correlation with the electric field in the calculations was performed using experimentally measured CV-curves [22,23].

2. Methods

2.1. DFT-calculations

For the DFT-calculations on the different Au surface morphologies SeqQuest [24,25], a periodic DFT program with localized basis sets represented by a linear combination of Gaussian functions, was used together with the PBE [26] generalized gradient approximation (GGA) exchange-correlation functional. A standard (non-local) norm-conserving pseudopotential [27] was applied to replace the 69 core electrons of each Au, leaving the 5d- and 6s-electrons in the valence space and invoking a nonlinear core correction [28]. The basis sets were optimized "double zeta plus polarization" contracted Gaussian functions.

All calculations were performed with nine-layer slabs, where the last three layers were fixed to the calculated bulk crystal structure ($a_0 = 4.164$ Å) while the remaining six layers were allowed to fully optimize their structure (to <0.01 eV/Å). Therefore, the reconstruction was only introduced to one side of the slab, and any artificial interslab dipole interactions were removed with the local moment counter charge method [29]. Finally, all calculations were performed with a converged Brillouin zone (BZ) sampling of 12 × 12 k-points for the 1 × 1 unitcell.

For studying the hexagonal reconstructed surface structure two different systems were used (see Fig. 1), a (5 × 1) and a (7 × 1) unitcell. Assuming a planar layer of hexagonal oriented atoms the (5 × 1) periodicity leads to a mismatch of 3.9%, which is only 2.6% with the (7 × 1) unitcell. To avoid any error from using different unitcells, we compared the surface free energy of Au(1 0 0)-(1 × 1) using a (1 × 1), (5 × 1), and a (7 × 1) unitcell, respectively. However, the surface free energies obtained with these three systems showed only negligible variations.

In order to introduce the presence of an electrode potential, a variable electric field was applied perpendicular to the surface. Since the slab was placed in the center of the unitcell the potential drop at the unitcell boundaries occurred in the vacuum region of the system and therefore caused no artificial influence on the Au-slabs. As a consequence of the electric field charge was moved from the bottom to the top layer. The resulting surface excess charge, which was needed to evaluate the surface free energies, was then obtained by integrating the difference charge density over the first two surface layers.

2.2. Thermodynamic considerations

In order to compare the stability of different surfaces the important quantity is the surface free energy (in electrochemistry often called surface tension):

$$\gamma(T, p, \phi_e) = \frac{1}{A}[G(T, p, N_{Au}, q^{exc}) - N_{Au}\mu_{Au}^{bulk}(T, p) - q^{exc}(\phi_e)\phi_e] \quad (1)$$

where A is the surface area (in case of the slab geometry both the top and bottom layers have to be considered), G the Gibbs free energy of the slab containing N_{Au} gold atoms, μ_{Au}^{bulk} the chemical potential of the Au-bulk reservoir, q^{exc} the excess surface charge and ϕ_e the electrode potential (with respect to a reference electrode). Using this equation it is assumed that the surface is in contact with an Au-bulk reservoir.

Since the ground-state bulk-structure of Au is an fcc-crystal, the chemical potential $\mu_{Au}^{bulk}(T, p)$ can be replaced by the Gibbs free energy per atom of the fcc-crystal $g_{Au}^{bulk}(T, p)$. In addition, because the Au bulk-reservoir and the Au-surfaces are present in the solid phase, it is reasonable to assume the T and p dependence of $G(T,p,N_{Au},q^{exc})$ and $g_{Au}^{bulk}(T, p)$ to be rather small, that is why the DFT-energies, which mimic $T = 0$ K, can be used instead. Therefore, G can be replaced by the total energy of the system, but without the energy contributions from the vacuum-electric-

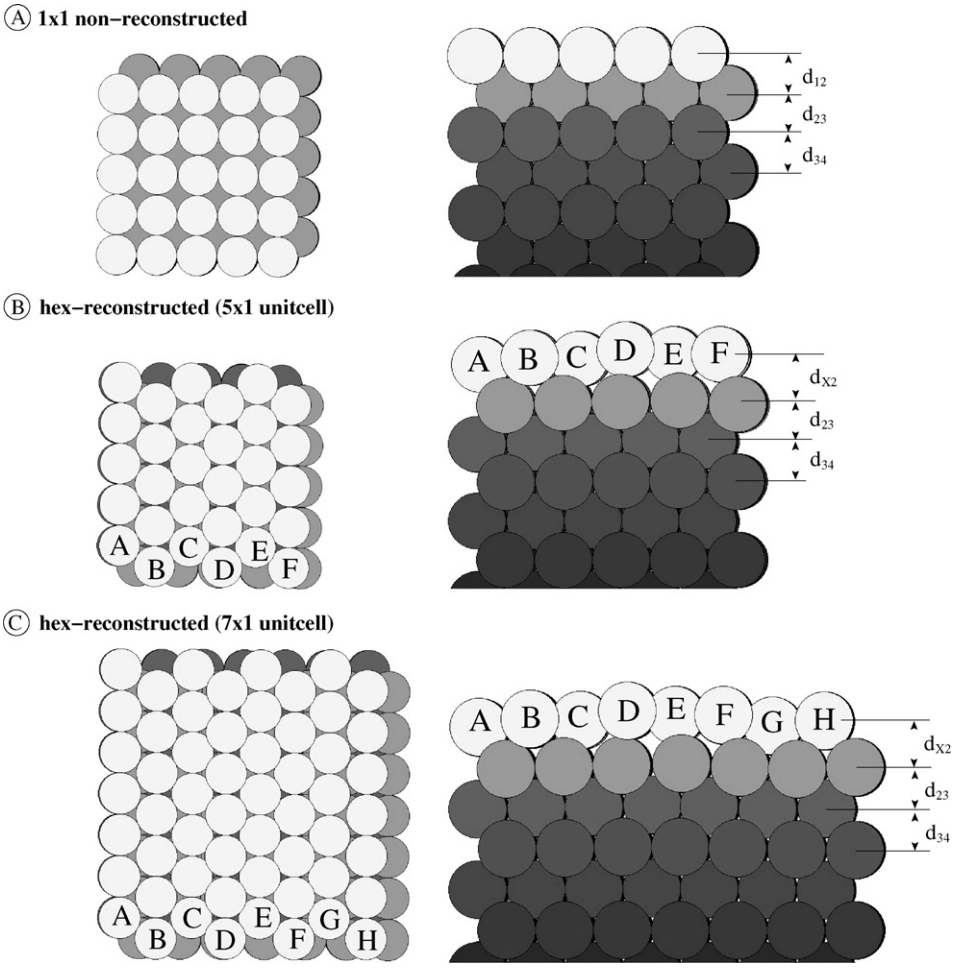

Fig. 1. Top and side views on the different unitcells used for the calculations (A) (1 × 1) non-reconstructed (bulk-truncated); (B) hexagonal-reconstructed with (5 × 1) periodicity; (C) hexagonal-reconstructed with (7 × 1) periodicity. In addition, atom and distance labels as used in Table 1 are given.

field (see also Ref. [2]), leading to the following equation:

$$\gamma(|\vec{E}|) = \frac{1}{A}[E_{\text{tot}}(|\vec{E}|) - N_{\text{Au}} g_{\text{Au}}^{\text{bulk}}] - \sigma^{\text{exc}} \mu_{\text{e}} \quad (2)$$

Since the presence of the electrode potential was modeled by applying an external electric field perpendicular to the surface, all potential-dependent terms in Eq. (1) are now dependent on the electric field. In addition, some changes were made on the last term of Eq. (1), which accounts for the energy required to transfer the potential-dependent excess charge $q^{\text{exc}}(\phi_{\text{e}})$ from the reference electrode to the gold surface. Firstly, the term has already been divided by the surface area A. This leads to the surface charge density σ^{exc}, which can easily be extracted from electronic structure calculations. Secondly, because the excess charge on the surface originates from the bottom layer the electrode potential was replaced by the chemical potential of the electrons on the surface (further discussion can be found in Section 3.2).

Finally we would like to remark that normally one has to use the interfacial free energy to study the stability of the electrode/electrolyte interface, which would result in some additional terms to Eq. (1). However, in our calculations we only considered the Au-surface without explicitly treating the electrolyte. Therefore, we were able to use the surface free energy instead.

3. Results and discussion

In the following we will first discuss the structural changes of both Au(1 0 0) surface morphologies when applying an external electric field. Afterwards the surface free energies will be evaluated, which then allow for a comparison of the stability.

3.1. Surface structure

The electric field directed perpendicular to the surface causes charge to be transferred within the periodic slab. Due to the metallic character of gold, this charge transfer mainly influences the bottom and top layers of the slab. As a result the electronic structure of the system changes, which in addition to the electrostatic repulsion of the excess charge gives rise to structural changes. Table 1 summarizes the interlayer distances for Au(1 0 0)-(1 × 1) and both Au(1 0 0)-hex surfaces in absence of any electric field and with relatively strong electric fields (±3.85 eV/Å) of opposite directions.

Table 1
Layer separations for the three systems as indicated in Fig. 1

System	Au(1 0 0)-(1 × 1)			Au(1 0 0)-hex (with 5 × 1 unitcell)			Au(1 0 0)-hex (with 7 × 1 unitcell)		
$\|\vec{E}\|$ (eV/Å)	−3.85	0.00	3.85	−3.85	0.00	3.85	−3.85	0.00	3.85
σ^{exc} (e/Å^2)	−0.022	0.00	0.021	−0.019	0.00	0.018	−0.020	0.00	0.019
d_{A2} (Å)	–	–	–	2.073	2.051	2.061	2.057	2.003	2.025
d_{B2} (Å)	–	–	–	2.498	2.405	2.438	2.604	2.430	2.513
d_{C2} (Å)	–	–	–	2.538	2.342	2.537	2.679	2.375	2.458
d_{D2} (Å)	–	–	–	3.026	2.851	3.067	3.014	2.844	2.904
d_{E2} (Å)	–	–	–	2.762	2.600	2.708	2.808	2.646	2.656
d_{F2} (Å)	–	–	–	2.658	2.573	2.788	2.752	2.619	2.792
d_{G2} (Å)	–	–	–	–	–	–	2.123	2.087	2.135
d_{H2} (Å)	–	–	–	–	–	–	2.390	2.355	2.363
d_{12} (Å)	2.155	2.052	2.106	–	–	–	–	–	–
d_{23} (Å)	2.132	2.076	2.149	2.126	2.057	2.148	2.130	2.061	2.134
d_{34} (Å)	2.135	2.085	2.149	2.133	2.071	2.161	2.142	2.077	2.147

For each system three different electric fields are considered: −3.85, 0.00, and 3.85 eV/Å. In addition, while all first-layer atoms of both hexagonal-reconstructed systems are distinguished, for all other layers an averaged value was calculated and used.

Without any electric field the non-reconstructed Au(1 0 0) surface shows only a small relaxation of the first (1.4%) and second (0.3%) surface layer, which is in agreement with experimental observations [30]. However, applying an electric field causes an increase of the layer separation. Accumulating negative charge at the surface the distance between the first two surface layers (d_{12}) increases by ≈0.10 Å (4.8% of the bulk value d^{bulk}), while d_{23} and d_{34} increase by 0.05–0.06 Å. Since changing the direction of the electric field, which now results in an accumulation of positive charge on the surface, also causes an increase of the interlayer distances, the main contributions seem to have their origin in the electrostatic repulsion. However, from that one would expect that, when moving from the surface towards bulk, the distance between the layers should converge to d^{bulk} (with no electric field). Instead it seems that the bulk lattice constant a_0 is not constant, but correlates with the change of the Fermi-level of the system resulting from the applied electric field. Consequently, the size of the unitcells used to model the different surfaces should also be adjusted with respect to the electric field. However, in our calculations the unitcells for the different surfaces were kept fixed at their bulk-truncated extension. Since the comparison between the d_{34}-values for the different surfaces but with the same electric field (see Table 1) show only minor variations, it is reasonable to assume that the stress introduced to the systems by not adjusting the unitcell should be comparable. Therefore, when evaluating surface stabilities these contributions should cancel out to a large extend.

Since for the reconstructed surfaces there is one additional atom per unitcell, the hexagonal structure of the first surface layer has to adjust to the underlying (1 × 1) geometry. In case of the (5 × 1) unitcell this leads to atom A (see Fig. 1B) occupying a four-fold position, while atom D is almost on top of an underlying gold atom. As a consequence, there is a slight buckling within the reconstruction layer in the range of 0.8 Å (no electric field). To ensure that we found the correct ground-state structure, we also performed a series of calculations in which the top layer was translated against the truncated (1 0 0) surface. The lowest energy structure obtained after geometry optimization is shown in Fig. 1B. After applying the relatively strong electric field (independent of the direction) the excess charge within the overlayer causes a slight lifting against the second surface layer. As expected the degree each atom of the overlayer is lifted correlates with the number of bonds it forms to second layer atoms. Having more bonds (e.g. atom A) allows for a better distribution of the excess charge compared to an on top bound atom (e.g. atom D). As a result, there is a stronger buckling ($d_{D2} - d_{A2} \approx 1.0$ Å) within the reconstructed layer than was observed without the electric field. This might already be an indication for the potential-induced lifting of the surface reconstruction.

Although the (7 × 1) unitcell provides more space for the reconstructed layer to adjust to the underlying bulk-truncated structure, we obtain a similar buckling as with the (5 × 1) unitcell (see Fig. 1C). However, besides atom A now atom G also occupies a four-fold-like surface site, leading to a position close to the second layer. Again the presence of the electric field enhances the surface buckling from 0.8 Å to around 1.0 Å.

3.2. Fcc-bulk crystal

While the geometrical changes have been discussed in the previous section, in this section we will analyze the electronic structure and the surface stability.

Under UHV conditions the ground state of the Au(1 0 0) surface is the hexagonal reconstruction configuration. Thus, without any external electric field the surface free energy of Au(1 0 0)-hex should be lower than the corresponding value of Au(1 0 0)-(1 × 1). Indeed, using the DFT calculated total energies and the calculated reference energy for Au in the fcc-bulk crystal structure, the surface free energy (using Eq. (2) without the last term) for the hexagonal-reconstructed surface is 0.002 eV/Å^2 (0.04 J/m^2) lower than that of Au(1 0 0)-(1 × 1). This difference is in perfect agreement with the value of 0.041 J/m^2 proposed by Santos and Schmickler [16] and with recent DFT-calculations by Feng et al. [2], who found 0.05 J/m^2 on the GGA-level. While our calculations mimic the case of

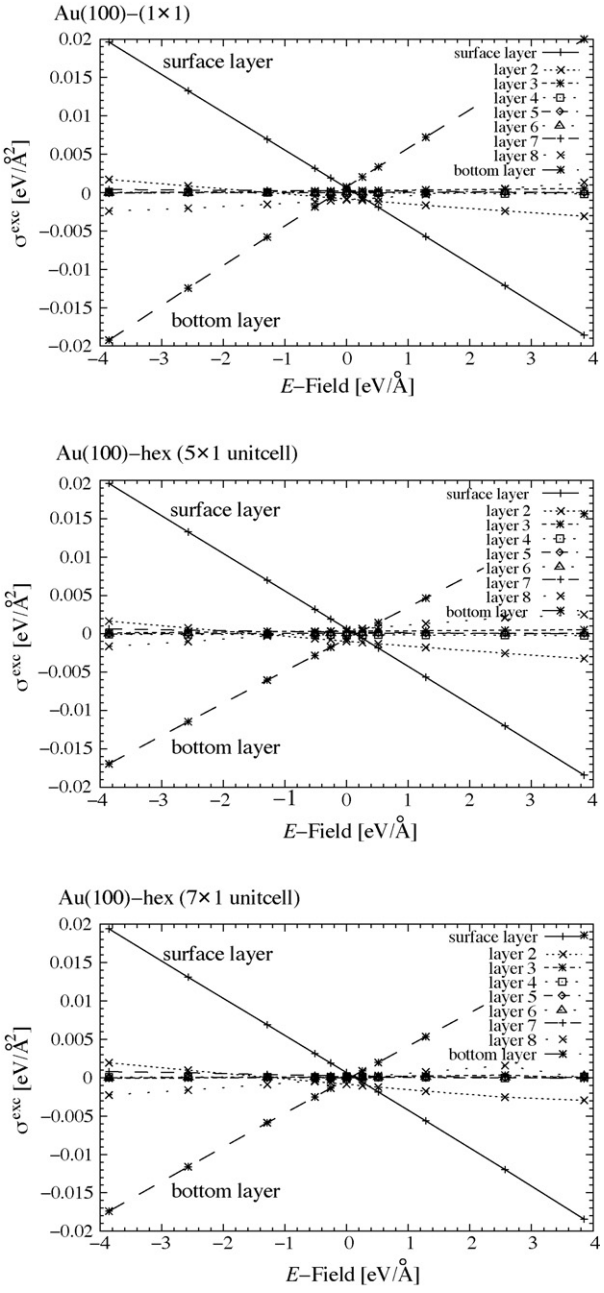

Fig. 2. Excess charge densities as function of the applied electric field. The layer-localization was performed by integrating over the charge distribution (nuclei and electron density) from the center between two layers over the slab-layer of consideration to the next center between two layers.

$T = 0$ K, this small difference in the surface stability already implies the ability of lifting the reconstruction by changing the external parameters, such as temperature or potential. However, it should also be remarked that such a small difference might be within the inaccuracy of current DFT calculations.

In order to obtain the surface free energy as function of the electrode potential, we afterwards applied an external field to the systems. As already mentioned, the field causes charge to move from the bottom layer to the top layer of the slab. Fig. 2 shows the net charge density per layer for the three systems studied as function of the applied electric field. The localization was performed by integrating the difference charge over parallel sheets, which in the direction parallel to the surface extended over the entire unitcell but in the other direction only over adjacent layer spacings. As expected for a metallic system the charge separation induced by the electric field mainly influences the bottom and top layer of the slab. However, there is also a small effect on the layers below both surface layers (layers 2 and 8). Therefore, the electrostatic repulsion causes the excess charge on the surface not to be aligned in a single, infinitely thin layer as classical models might imply, but to form a thin, diffuse distribution at the surfaces. Moreover, while the excess charge in the top and bottom layers changes linearly with the electric field, there is a slight curvature for the underlying layers. In addition, the plots in Fig. 2 show that with no electric field there is a net charge at the surface, and only by applying a finite field, which should correspond to the potential of zero charge (psz), this net charge can be removed.

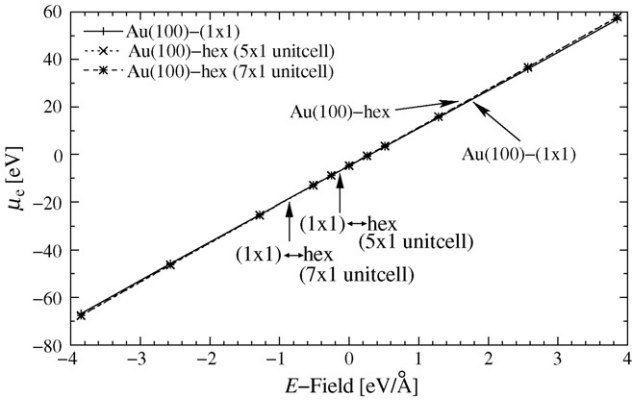

Fig. 3. Chemical potential of the electrons on the surface of each system as a function of the applied electric field. At positive electrode potentials the curve of Au(1 0 0)-hex lies above the curve of Au(1 0 0)-(1 × 1).

Comparing the charge density distribution for the reconstructed and non-reconstructed surfaces also shows that while for Au(1 0 0)-(1 × 1) the curves for the bottom and surface layer are almost symmetric around $\sigma^{exc} = 0\,eV/Å^2$, the additional surface atom in both Au(1 0 0)-hex systems breaks this symmetry and allows higher charge densities in the topmost layer.

Similar to the charge density distribution the chemical potential of the electrons on the surface:

$$\mu_e = \varepsilon_{Fermi} - V_{eff}\,(\text{bottom}) \tag{3}$$

also changes linearly with the electric field (see Fig. 3). Usually μ_e refers to the energy to move an electron from the Fermi energy of the electrode to infinity. However, due to the periodic approach that is used within the present studies, infinity is not well defined. Instead the excess charge on the electrode surface originates from the bottom layer, that is why μ_e is obtained as the difference between the Fermi-level ε_{Fermi} of the system (electrode) and the Kohn–Sham effective potential (V_{eff}) at the bottom layer of the slab (Eq. (3)). This observed linear behavior is in agreement with earlier studies by Lozovoi et al. on charged periodic systems [31]. However, for their calculations on the surface stability of Au(1 1 0) and Pt(1 1 0) [32] they used a symmetric system and placed a reference electrode in the middle of

the vacuum region to account for the excess charge added to the slab. Therefore, to evaluate μ_e they took the effective potential at the reference electrode. Also in agreement with their findings, the μ_e-curves show a transition at small negative electric fields, which correspond to a negative excess charge on the surface. However, since the curves have almost identical slopes, this only allows a qualitative statement.

On the basis of the total energies, the surface charge densities σ^{exc}, and the electron chemical potentials, which have been calculated for different electric fields, Eq. (2) was used to evaluate the surface energy γ of the non-reconstructed and both reconstructed surfaces as function of the electric field applied in the calculation. However, in order to allow for a comparison between the different surfaces and with the experimental observations, the necessary functionality would be γ as a function of the electrode potential (U_{SCE}) instead of the electric field. The problem here is that the electric field influences each of the surfaces in a different way, as can be seen in the behavior of the surface charge density on Au(1 0 0)-(1 × 1) and Au(1 0 0)-hex (Fig. 2). Moreover, in the realistic system the gold electrode is in contact with an electrolyte, which determines the structure of the electric double-layer and therefore the potential drop. Thus, it is obvious that changing the ion concentration results in a different double-layer structure. As a consequence the charge accumulated at the electrode surface also changes. In order to include these effects it would be necessary to simulate the entire electrode/electrolyte interface self-consistently, allowing the surface excess charge and the ion distribution within the electric double layer to adjust itself. However, the system sizes required to model the complete interface very much exceed the capabilities of actual *ab initio* methods, which are necessary to reproduce the small energy differences between both surface configurations of Au(1 0 0).

In order to include the effects of the electrolyte and to evaluate surface free energies on the same reference, we correlated our calculated $\sigma^{exc}(|\vec{E}|)$ curves with experimentally extracted $\sigma^{exc}(|U_{SCE}|)$-curves [22,23]. This enabled us to replace the electric field-scale with the experimentally obtained U_{SCE}-scale. Doing this for each surface structure separately we obtained the surface free energies as function of the (experimentally) applied electrode potential. Fig. 4 shows the so-obtained surface free energies as function of the electrode potential U_{SCE} for two different electrolyte concentrations. With a low electrolyte concentration of 0.01 M $HClO_4$, we find a transition from the hexagonal-reconstructed to the non-reconstructed structure at ≈+0.6 V. While below this potential value the thermodynamically stable phase is the Au(1 0 0)-hex surface, above this potential Au(1 0 0)-(1 × 1) becomes more stable. Increasing the electrolyte concentration to 0.1 M $HClO_4$ shows a similar behavior, but the potential value at which the transition occurs is approximately 0.1 V lower. As expected from similar surface structures and σ^{exc}-dependencies, the comparison between both surface free energy-curves obtained with the (5 × 1) and the (7 × 1) unitcell shows only minor deviations.

Since only electronic effects and no specific ion adsorption has been considered in our calculations, from the agreement of our calculated transition potential between +0.5 and +0.6 V (depending on the electrolyte concentration) with the experimentally measured value one might conclude, that the lifting of the Au(1 0 0)-hex surface reconstruction is caused by the surface charging only. However, since up to now modeling of the full electric double-layer is not possible, experimentally measured CV-curves were required as external input. As the occurrence of any specific ion adsorption should already influence the experimental CV-curves, from our studies and similar calculations by other groups, specific adsorption cannot be excluded. Instead the results give evidence that surface charging alone already plays an important role in destabilizing the hexagonal-reconstructed Au(1 0 0) surface at positive potentials.

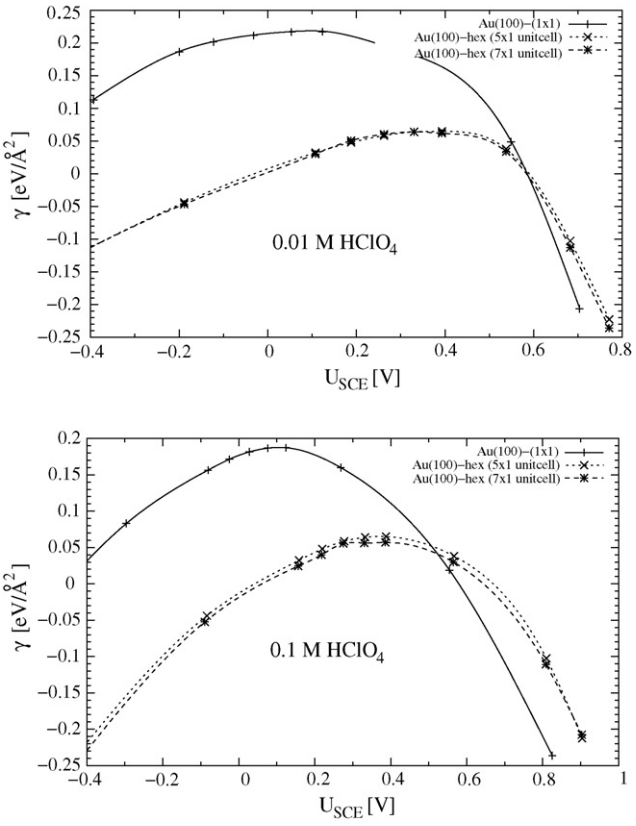

Fig. 4. Surface free energies as function of the electrode potential (ref. SCE-electrode). The upper plot shows the stability of the different Au(1 0 0)-surfaces in a 0.01 M $HClO_4$ electrolyte, while the lower plot corresponds to a higher ion concentration of 0.1 M $HClO_4$.

4. Summary and outlook

Density functional theory calculations were performed to study the surface stability of the non-reconstructed and hexagonal-reconstructed Au(1 0 0) surfaces. Without any external electric field we found a slightly lower surface energy for Au(1 0 0)-hex, which is in agreement with UHV-experiments that find the hexagonal-reconstructed surface structure to be the ground state.

Since bringing the Au-electrode in contact with an electrolyte of weakly adsorbing ions (e.g. $HClO_4$) and applying a potential positive with respect to the potential of zero charge causes a lifting of the reconstructed surface, we afterwards calculated the surface stability as function of an external electric field. The

surface free energy-curves, which were obtained after correlating our surface charge densities to those extracted from CV-measurements, already show the phase-transition. The potential at which the transition from Au(1 0 0)-hex to Au(1 0 0)-(1 × 1) occurs was calculated to be +0.6 V for low (0.01 M $HClO_4$) and +0.5 V for higher ion concentrations (0.1 M $HClO_4$) in the electrolyte, what is in agreement with the experimental observation by Kolb et al.

While our calculations indicate that surface charging due to the electrode potential alone already plays a major role in lifting the surface reconstruction, specific ion adsorption cannot be excluded. Forthcoming calculations, which will model the entire electrode/electrolyte interface self-consistently, will be able to answer this question.

Acknowledgements

Support by the German academic exchange service (DAAD) and the "Fonds der Chemischen Industrie" (VCI) is greatly acknowledged.

References

[1] D.M. Kolb, Prog. Surf. Sci. 51 (1996) 109.
[2] Y.J. Feng, K.P. Bohnen, C.T. Chan, Phys. Rev. B 72 (2005) 125401.
[3] D.G. Fedak, N.A. Gjostein, Phys. Rev. Lett. 16 (1966) 171.
[4] K.H. Rieder, T. Engel, R.H. Swendsen, M. Manninen, Surf. Sci. 127 (1983) 223.
[5] D.G. Fedak, N.A. Gjostein, Surf. Sci. 8 (1967) 77.
[6] J.F. Wendelken, D.M. Zehner, Surf. Sci. 71 (1978) 178.
[7] M.A. van Hove, R.J. Koestner, P.C. Stair, J.P. Biberian, L.L. Kesmodel, I. Bartos, G.A. Somorjai, Surf. Sci. 103 (1981) 189.
[8] G.K. Binnig, H. Rohrer, C. Gerber, E. Stoll, Surf. Sci. 144 (1984) 321.
[9] D. Tomanek, K.H. Bennemann, Surf. Sci. 163 (1985) 503.
[10] F. Ercolessi, E. Tosatti, M. Parrinello, Phys. Rev. Lett. 57 (1986) 719.
[11] B.W. Dodson, Phys. Rev. B 35 (1987) 880.
[12] N. Takeuchi, C.T. Chan, K.M. Ho, Phys. Rev. B 43 (1991) 14363.
[13] D.M. Kolb, J. Schneider, Surf. Sci. 162 (1985) 764.
[14] D.M. Kolb, J. Schneider, Electrochim. Acta 31 (1986) 929.
[15] J. Schneider, D.M. Kolb, Surf. Sci. 193 (1988) 579.
[16] E. Santos, W. Schmickler, Chem. Phys. Lett. 400 (2004) 26.
[17] M.I. Haftel, Phys. Rev. B 48 (1993) 2611.
[18] M.I. Haftel, M. Rosen, Phys. Rev. B 64 (2001) 195405.
[19] M.I. Haftel, M. Rosen, Surf. Sci. 523 (2003) 118.
[20] Y.J. Feng, K.P. Bohnen, C.T. Chan, Phys. Rev. B 72 (2005) 125401.
[21] K.P. Bohnen, D.M. Kolb, Surf. Sci. 407 (1998) L629.
[22] D.M. Kolb, J. Schneider, Surf. Sci. 221 (1985) 764.
[23] D. Eberhardt, E. Santos, W. Schmickler, J. Electroanal. Chem. 419 (1996) 23.
[24] P.A. Schultz, A description of the method is in: P.J. Feibelman, Phys. Rev. B 35 (1987) 2626, unpublished data.
[25] C. Verdozzi, P.A. Schultz, R. Wu, A.H. Edwards, N. Kioussis, Phys. Rev. B 66 (2002) 125408.
[26] J.P. Perdew, K. Burke, M. Ernzerhof, Phys. Rev. Lett. 88 (1996) 3865.
[27] D.R. Hamann, Phys. Rev. B 40 (1989) 2980.
[28] S.G. Louie, S. Froyen, M.L. Cohen, Phys. Rev. B 26 (1982) 1738.
[29] P.A. Schultz, Phys. Rev. B 60 (1999) 1551.
[30] Ch. Kittel, Einführung in die Festkörperphysik, R. Oldenbourg Verlag, München, 1991.
[31] A.Y. Lozovoi, A. Alavi, J. Kohanoff, R.M. Lynden-Bell, J. Chem. Phys. 115 (2001) 1661.
[32] A.Y. Lozovoi, A. Alavi, Phys. Rev. B 68 (2003) 245416.